

See discussions, stats, and author profiles for this publication at: <https://www.researchgate.net/publication/12188000>

High-Resolution Near-Infrared Imaging of DNA Microarrays with Time-Resolved Acquisition of Fluorescence Lifetimes

ARTICLE *in* ANALYTICAL CHEMISTRY · JANUARY 2001

Impact Factor: 5.64 · DOI: 10.1021/ac0009705 · Source: PubMed

CITATIONS

74

READS

31

8 AUTHORS, INCLUDING:



Emanuel Waddell

University of Alabama in Huntsville

32 PUBLICATIONS 411 CITATIONS

SEE PROFILE

High-Resolution Near-Infrared Imaging of DNA Microarrays with Time-Resolved Acquisition of Fluorescence Lifetimes

Emanuel Waddell,[†] Yun Wang, Wieslaw Stryjewski, Scott McWhorter, Alyssa C. Henry, David Evans,[‡] Robin L. McCarley,^{*} and Steven A. Soper^{*}

Louisiana State University, Department of Chemistry, Baton Rouge, Louisiana 70803-1804

Ultrasensitive, near-infrared (NIR), time-resolved fluorescence is evaluated as a detection method for reading DNA hybridization events on solid surfaces for microarray applications. In addition, the potential of multiplexed analyses using time-resolved identification protocols is described. To carry out this work, a NIR time-resolved confocal imager was constructed to read fluorescence signatures from the arrays. The device utilized a 780-nm pulsed diode laser, a single-photon avalanche diode (SPAD), and a high-numerical-aperture microscope objective mounted in an epi-illumination format. Due to the small size of the components that are required to construct this imager, the entire detector could easily be mounted on high-resolution translational stages and scanned over the stationary arrays. The instrument response function of the device was determined to be 275 ps (fwhm), which is adequate for measuring fluorophores with subnanosecond lifetimes. To characterize the system, NIR dyes were deposited directly on different substrate materials typically used for DNA microarrays, and the fluorescence lifetimes of two representative dyes were measured. The fluorescence lifetime for aluminum tetra-sulfonated naphthalocyanine was found to be 1.92 ns, and a value of 1.21 ns was determined for the tricarbo-cyanine dye, IRD800, when it was deposited onto poly(methyl methacrylate) (PMMA) and measured in the dry state. Finally, the imager was used to monitor hybridization events using probe oligonucleotides chemically tethered to a PMMA substrate via a glutardialdehyde linkage to an aminated-PMMA surface. The limit of detection for oligonucleotides containing a NIR fluorescent reporter was determined to be 0.38 molecules/ μm^2 , with this detection limit improving by a factor of 10 when a time-gate was implemented. Fluorescence lifetime analysis of the hybridization events on PMMA indicated a lifetime value of 1.23 ns for the NIR-labeled oligonucleotides when using maximum-likelihood estimators.

DNA microarrays are becoming an ubiquitous tool for probing DNA structure in both research and clinical applications. Micro-

arrays have assumed immense popularity due to the highly parallel nature in which they are constructed and operated.¹ In most DNA microarray examples, the material that is tethered to the solid support can be a short oligonucleotide probe (<100 nt, format II) or an intact DNA target (>100 nt, format I). The applications that have used DNA microarrays include expression profiling,² de novo sequencing,³ and DNA variation on a genome-wide scale.⁴

When short oligonucleotides are immobilized to the solid support, the attachment and/or construction of the probes can be accomplished using one of two methods. In the first, a photolithographic method is used to perform solid-phase DNA synthesis with phosphoramidite chemistry and photochemical deprotecting groups.^{2,5} Using this light-generated synthesis method, high-density arrays (pixel size, $\sim 2\ \mu\text{m}$) can be produced using minimal synthetic steps (number of steps = $4n$, where n is the length of the synthetic DNA probe). In the second method, inkjet technology is used to actually "print" specific oligonucleotide probes which have been pre-synthesized and purified using standard procedures at different locations on the array and are tethered covalently to the support.^{6–8} When intact DNAs are immobilized onto the solid support, various types of substrates are used to allow covalent interactions between the DNA and support material. Examples of materials that are used in these applications include poly-L-lysine-coated glass slides or nylon membranes.

In most cases, the common support material that is used for high-density microarrays is glass. The properties of glass that make it an attractive substrate for DNA arrays include its (1)

- (1) Collins, F. S. *Nat. Genet.* **1999**, *21*, 2.
- (2) Lipshutz, R. J.; Fodor, S. P. A.; Gingeras, T. R.; Lockhart, D. J. *Nat. Genet.* **1999**, *21*, 20–24.
- (3) Hacia, J. G.; Fan, J. B.; Ryder, O.; Jin, L.; Edgemon, K.; Ghandour, G.; Mayer, R. A.; Sun, B.; Hsie, L.; Robbins, C. M.; Brody, L. C.; Wang, D.; Lander, E. S.; Lipshutz, R.; Fodor, S. P. A.; Collins, F. S. *Nat. Genet.* **1999**, *22*, 164–167.
- (4) Cargill, M.; Altshuler, D.; Ireland, J.; Sklar, P.; Ardlie, K.; Patil, N.; Lane, C. R.; Lim, E. P.; Kalyanaraman, N.; Nemes, J.; Ziaugra, L.; Friedland, L.; Rolfe, A.; Warrington, J.; Lipshutz, R.; Daley, G. Q.; Lander, E. S. *Nat. Genet.* **1999**, *22*, 231–238.
- (5) (a) Pease, A. C.; Solas, D.; Sullivan, E. J.; Cronin, M. T.; Holmes, C. P.; Fodor, S. P. A. *PNAS* **1994**, *91*, 5022–5026. (b) Chee, M.; Yang, R.; Hubbell, E.; Berno, A.; Huang, X. C.; Stern, D.; Winkler, J.; Lockhart, D. J.; Morris, M. S.; Fodor, S. P. A. *Science* **1996**, *274*, 610–614.
- (6) Guo, Z.; Guilfoyle, R. A.; Thiel, A. J.; Wang, R.; Smith, L. M. *Nucleic Acids Res.* **1994**, *22*, 5456–5465.
- (7) Shalon, D.; Smith, S. J.; Brown, P. O. *Genome Res.* **1996**, *6*, 639–645.
- (8) Brown, P. O.; Botstein, D. *Nat. Genet.* **1999**, *21*, 33–37.

[†] Present address: National Institute of Standards and Technology (NIST), Gaithersburg, MD.

[‡] Permanent address: Radius Biosciences, Medfield, MA.

impermeability, which speeds up the kinetics of hybridization by keeping the hybridization volume small; (2) high rigidity, making it easy to image; (3) robust immobilization chemistries to allow covalent linkage of oligonucleotides to the solid-support; and (4) low background fluorescence when high-intensity lasers are focused onto its surface, improving the signal-to-noise ratio (SNR) in the measurement when fluorescence is used for readout.

Unfortunately, there are some severe limitations when incorporating glass as the substrate material for microarrays, namely, the limited surface density of functional groups for immobilizing targets due to its impermeability (2-dimensional measurement). For example, in glass, the surface concentration of the tethered oligonucleotides is determined by the density of the functional groups (silanols), which is $\sim 10^{-10}$ moles/cm². Due to steric considerations and the inefficiency of hybridization, the surface concentration of accessible oligonucleotides is 1 molecule/500 Å², which results in a required detection level of $\sim 6\,500$ molecules/μm² for readout strategies using visible or far-red fluorescence.⁶ The situation is even more severe in cDNA arrays, due to further steric considerations and extremely poor hybridization efficiency, producing on average 0.0012 fluors/μm² from each target hybridized to its tethered probe.⁹

The commonly used transduction mode for reading microarrays is fluorescence, due to its superior limit of detection and the ability to monitor multiple reporter molecules simultaneously (multiplexed applications). In the case of fluorescence, a dye is either covalently attached to the 5' end of the probe used to interrogate the array or to dUTP analogues that are incorporated during reverse transcription (cDNA arrays). Absolute intensity may then be used to determine whether selective binding of the probe to the immobilized target occurred. The common dyes that are used for interrogating DNA microarrays include Cy3 ($\lambda_{\text{ex}} = 514$ nm) and Cy5 ($\lambda_{\text{ex}} = 632$ nm).^{9–11} The choice of these dyes is due to their favorable photochemical stabilities and quantum yields, well-resolved emission profiles, and the fact that dUTP analogues of Cy3 and Cy5 are readily incorporated during reverse transcription.⁹

In many applications, in particular format I-type hybridization assays, it becomes necessary to screen for multiple probes that are hybridizing to a single target tethered to the substrate. In addition, differential expression assays, which report on the relative abundance of particular genes, require dual labeling of reverse-transcribed DNA labeled with unique reporter molecules. In these cases, it is common to use wavelength-discrimination methods to effectively identify whether the probe(s) hybridized to the target DNA found at a specific location in the array. However, the number of probes that can be effectively identified is limited by the broad emission profiles associated with most molecular chromophore systems.

Recently, fluorescence lifetimes have been proposed as an alternative to wavelength discrimination in multiplexed applications, specifically in DNA sequencing.^{12–22} Implementation of lifetime discrimination into a multiplexed application could po-

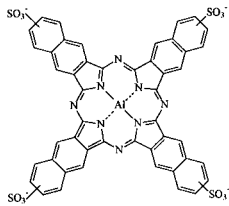
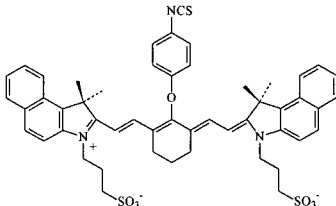
tentially allow for the use of only one readout channel (one laser and one photodetector) but still possess the ability to monitor many different fluorescent labels when the reporters have similar absorption and emission profiles but distinguishable lifetimes. The common approach for acquiring lifetimes of fluorophores, especially in the limit of poor photon statistics, has been the use of time-correlated single photon counting (TCSPC), which uses a pulsed laser and the appropriate electronics. The advantages of TCSPC are its broad dynamic range, single photon sensitivity, and favorable time-resolution that can be achieved when appropriate instrumental components are used.²³ Additionally, TCSPC can minimize background signals in the form of scatter by time-gating, which processes only those photons that are produced during a pre-selected time window. Therefore, scattering photons that are coincident with the laser pulse can be gated out of the observed signal, which improves the SNR.^{24,25}

Near-infrared (NIR) fluorescence monitoring can be particularly attractive for lifetime-based applications for which high sensitivity is required.^{13,26–28} One of the primary advantages of NIR fluorescence includes the minimal amount of background signals it produces, which can improve the precision and accuracy in a lifetime measurement.^{29,30} In addition, the instrumentation used in the NIR can be much simpler than that required for visible time-resolved fluorescence measurements.¹⁴ Therefore, when using NIR fluorescence, robust and simple TCSPC devices can be constructed that exhibit high sensitivity, are capable of simple operation, and can be configured in a footprint that can be easily scanned for imaging applications.

- (9) Duggan, D. J.; Bittner, M.; Chen, Y.; Meltzer, P.; Trent, J. M. *Nat. Genet.* **1999**, *21*, 10–14.
- (10) Gallardo, B. S.; Gupta, V. K.; Eagerton, F. D.; Jong, L. I.; Craig, V. S.; Shah, R. R.; Abbott, N. L. *Science* **1999**, *283*, 57.
- (11) Lin, V. S.-Y.; Motesharei, K.; Dancil, K.-P. S.; Sailor, M. J.; Ghadari, M. R. *Science* **1997**, *278*, 840–843.

- (12) Bachteler, G.; Drexhage, K. H.; Ardenjacob, J.; Han, K. T.; Kollner, M.; Muller, R.; Sauer, M.; Seeger, S.; Wolfrum, J. *J. Lumin.* **1994**, *62*, 101–108.
- (13) Soper, S. A.; Legendre, B. L.; Williams, D. C. *Anal. Chem.* **1995**, *67*, 4358–4365.
- (14) Legendre, B. L.; Williams, D. C.; Soper, S. A.; Erdmann, R.; Ortmann, U.; Enderlein, J. *Rev. Sci. Instr.* **1996**, *67*, 3984–3989.
- (15) Kollner, M.; Fischer, A.; Ardenjacob, J.; Drexhage, K. H.; Muller, R.; Seeger, S.; Wolfrum, J. *Chem. Phys. Lett.* **1996**, *250*, 355–360.
- (16) Li, L. C.; McGowen, L. B. *Anal. Chem.* **1996**, *68*, 2737–2743.
- (17) Li, L. C.; He, H.; Nunnally, B. K.; McGowen, L. B. *J. Chromatogr. B* **1997**, *695*, 85–92.
- (18) Lieberwirth, U.; Arden-Jacob, J.; Drexhage, K. H.; Herten, D. P.; Muller, R.; Neumann, M.; Schulz, A.; Siebert, S.; Sagner, G.; Klingel, S.; Sauer, M.; Wolfrum, J. *Anal. Chem.* **1998**, *70*, 4771–4779.
- (19) Muller, R.; Zander, C.; Sauer, M.; Deimel, M.; Ko, D. S.; Siebert, S.; Ardenjacob, J.; Deltau, G.; Marx, N. J.; Drexhage, K. H.; Wolfrum, J. *Chem. Phys. Lett.* **1996**, *262*, 716–722.
- (20) Muller, R.; Herten, D. P.; Lieberwirth, U.; Neumann, M.; Sauer, M.; Schulz, A.; Siebert, S.; Drexhage, K. H.; Wolfrum, J. *Chem. Phys. Lett.* **1997**, *279*, 282–288.
- (21) Flanagan, J. H.; Owens, C. V.; Romero, S. E.; Waddell, E.; Kahn, S. H.; Hammer, R. P.; Soper, S. A. *Anal. Chem.* **1998**, *70*, 2676–2684.
- (22) Lassiter, S. J.; Strykowski, W.; Legendre, B. L.; Erdmann, R.; Wahl, M.; Wurm, J.; Peterson, R.; Middendorf, L.; Soper, S. A. *Anal. Chem.* (accepted for publication, 2000).
- (23) Lakowicz, J. R. *Topics in Fluorescence Spectroscopy*; Plenum Press: New York, 1992.
- (24) Soper, S. A.; Mattingly, Q. L.; Vegunta, P. *Anal. Chem.* **1993**, *65*, 740–747.
- (25) Shera, E. B.; Seitzinger, N. K.; Davis, L. M.; Keller, R. A.; Soper, S. A. *Chem. Phys. Lett.* **1990**, *174*, 553–557.
- (26) Legendre, B. L.; Soper, S. A. *Appl. Spectrosc.* **1996**, *50*, 1196–1202.
- (27) Flanagan, J. H.; Legendre, B. L.; Hammer, R. P.; Soper, S. A. *Anal. Chem.* **1995**, *67*, 341–347.
- (28) Soper, S. A.; Legendre, B. L. *Appl. Spectrosc.* **1998**, *52*, 1–6.
- (29) Tellinghulsen, J.; Goodwin, P. M.; Ambrose, W. P.; Martin, J. C.; Keller, R. A. *Anal. Chem.* **1994**, *66*, 64–72.
- (30) Soper, S. A.; Legendre, B. L. *Appl. Spectrosc.* **1994**, *48*, 400–405.

Table 1. Chemical Structures and Photophysical Properties of Two NIR Fluorescent Dyes Used in This Work

Photophysical Property	Al-Naphthalocyanine	IRD800
		
Absorption maximum (nm)	769	782
Emission maximum (nm)	781	810
Quantum yield	0.25	0.15
Fluorescence Lifetime (ns)	2.92	0.76
Photobleaching Quantum Yield	5.0×10^{-7}	1.7×10^{-6}
Photon yield per molecule	5.0×10^5	8.8×10^4

All photophysical properties were measured in DMSO.

In this manuscript, we discuss the use of time-resolved NIR fluorescence for reading signatures from DNA microarrays. The fluorescence produced from two representative NIR dyes, IRD800 (tricyanocyanine) and aluminum tetrasulfonated naphthalocyanine ($\text{AlNc}(\text{SO}_3^-)_4$, (see Table 1) were evaluated following the deposition of the material onto different substrates appropriate for microarray applications. In addition, to obtain the time-resolved fluorescence, a high-resolution (spatial and temporal) NIR-TCSPEC scanner was developed, and the operational characteristics of this device will be reported. We will also discuss the use of unique polymer materials, in particular, poly(methyl methacrylate) (PMMA), as a support substrate to which oligonucleotide probes can be tethered for microarrays due to the low background signals this polymer generates in the NIR. Finally, the application of NIR time-resolved confocal imaging for reading both steady-state and time-resolved fluorescence from DNA microarrays will be demonstrated.

EXPERIMENTAL SECTION

Chemicals and Substrates. All chemicals and solvents were purchased from Aldrich (Milwaukee, WI) and were used as received. The NIR dyes used for these studies, IRD800 (Li-COR Biotechnology, Lincoln, NE) and aluminum tetrasulfonated naphthalocyanine ($\text{AlNc}(\text{SO}_3^-)_4$, Porphyrin Products, Inc., Logan, UT) were used as received. Typically, stock solutions (0.1 mM) of the dyes were made in DMSO and stored in a refrigerator (4 °C) until required for use. The oligonucleotides used for hybridization assays were purchased from Midland Certified Reagent Company (Midland, TX) and consisted of a 5' amino modified end with a sequence of 5'- $\text{H}_2\text{N}(\text{CH}_2)_6\text{-TTTTTTTTTTTTTTGTCGTTTAA-CAAACGTCGTG-3'}$. The tethered oligonucleotide probe also contained a poly(dT)₁₅ linker to spatially remove the probe from the surface to improve its accessibility for hybridization.⁶ The complement, which contained an NIR label (IRD-800, Li-COR)

possessed the following sequence: IRD800-5'-CACGACGTTTG-TAAAACGAC-3'. PMMA was obtained from Goodfellow (Berwyn, PA). Precleaned glass microscope slides and microscope cover slips were purchased from Fisher Scientific (Pittsburgh, PA). Glass slides coated with poly-L-lysine were secured from Sigma Diagnostics (St. Louis, MO). The glass and PMMA slides were washed with methanol and dried in air prior to use. The poly-L-lysine coated slides were used as received.

Instrumentation. Previously, we described a scanner for time-resolved NIR fluorescence which utilized a large photoactive-area single-photon avalanche diode (SPAD, passively quenched) in conjunction with a 780-nm pulsed diode laser integrated onto a microscope head.³¹ This system was configured such that the laser was positioned at Brewster's angle with respect to the collection lens. The scanner had subnanosecond timing resolution, but possessed a large spot size (20 μm along the minor axis and 30 μm along the major axis) and a relatively poor f/#, which resulted in minimal collection of the fluorescence. Unfortunately, this scanner was not appropriate for the present application due to the large spot size of the laser and the poor collection efficiency of the relay optics. Therefore, we constructed a confocal imager with time-resolved capabilities and an improved collection efficiency.

NIR TCSPC measurements were made from the arrays using a device built in-house which consisted of a pulsed diode laser (PicoQuant GmbH, model 800, Berlin, Germany), a TCSPC board (PicoQuant GmbH, model SPC 430, Berlin, Germany), and a single-photon avalanche diode (SPAD, EG&G Optoelectronics, model SPCM-PQ, Vaudreuil, Canada). As Figure 1 depicts, the components were mounted with the aid of a mounting cube and lens tubes purchased from Thorlabs (Newton, NJ) and configured in an epi-illumination format. In addition, a circular aperture was

(31) Zhang, Y. L.; Soper, S. A.; Middendorf, L. R.; Wurm, J. A.; Erdmann, R.; Wahl, M. *Appl. Spectrosc.* **1999**, *53*, 497–504.

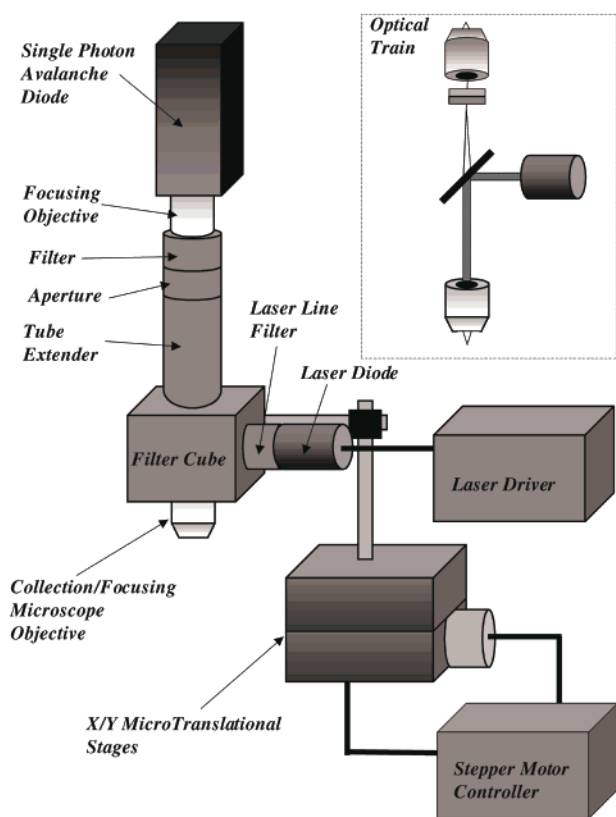


Figure 1. Schematic drawing of time-resolved NIR imager.

placed in the secondary image plane of the objective to allow implementation of confocal imaging when required.

The pulsed diode laser operated at a wavelength of 780 nm, a repetition rate adjustable from single shot to 80 MHz, and a temporal pulse width of approximately 50 ps (fwhm) with 7.5 mW of average power. An integrated optics set was provided with the laser to produce an elliptically shaped collimated output. The laser excitation beam was passed through a 780-nm line filter (Omega Optical, 780DF10, Brattleboro, VT), reflected by a dichroic filter (Omega Optical, 795DRLP), and focused onto the array surface using a 40X high-numerical-aperture (NA) microscope objective (Nikon, Natick, MA; NA = 0.85). The $1/e^2$ spot size was measured to be 3 μm (minor axis) by 5 μm (major axis). The fluorescence excitation was collected by the same microscope objective and transmitted through the dichroic, a circular aperture set at 2.0 mm (clear diameter), and finally through a filter stack consisting of a long-pass filter (cut on wavelength = 830 nm, Newport Corporation, Irvine, CA) and a band-pass filter centered at 825 nm (825RDF30, Omega Optical). After passing through the filters, the fluorescence was sent through a condensing lens (01LAG111/076, Melles Griot) and focused onto the SPAD. The passively quenched SPAD possessed a photoactive area of approximately 180 μm in diameter.

The entire fluorescence detector was mounted on an x/y microtranslational stage, which was controlled by stepper motors interfaced to a PC computer. The time-resolved data was accumulated on an IBM-compatible computer, which required digital pulses from the SPAD to construct both intensity and lifetime images. A standard NIM pulse was generated for each photoelectron event that fed the TCSPC board. The controlling computer contained the TCSPC board (PicoQuant SPC-430 module). The

SPC-430 provided up to 4096 time channels for each of 128 separately measured decay curves. The two onboard memory banks on the SPC-430 card allowed simultaneous transfer/collection of the data. Two bipolar stepper motors interfaced to the PC using STP-100 stepper motor controller boards obtained from Pontech, Inc. (Upland, CA) drove the x and y directions of the micro-translational stages. Each STP-100 was equipped with the RS-485 interface, which allowed full duplex, multi-drop communication with the host computer. A PP232-485f interface (Pontech, Inc.) was used to convert RS485 into the PC's RS232 protocol. Hall sensors were used to monitor the travel limits of the x/y stages. The step resolution of these stages was 12.7 μm with a scan range of 4 cm in both the x and y coordinates. The scanner operated by taking a single step and then acquiring the fluorescence data for a software-selectable integration period (10 ms – 10 s).

The data acquisition software was written in Visual Basic and consisted of several control and data acquisition functions, such as recording the position of the scanning head, streaming data (both intensity and time-resolved) to the hard drive, and providing real-time visualization of the acquired images. During a typical experiment, 4–12 GB of data were generated and stored in chunks of 2 GB. After imaging the array, the data was compressed one scan line at a time and subsequently assembled into one contiguous file. Additionally, the images of the intensity and calculated on-the-fly lifetimes for each pixel were stored in a separate file with no compression. During the data analysis, each line was read and decompressed separately for generation of the 2D image. This approach allowed manageable data file sizes at the expense of slightly longer time access to the information.

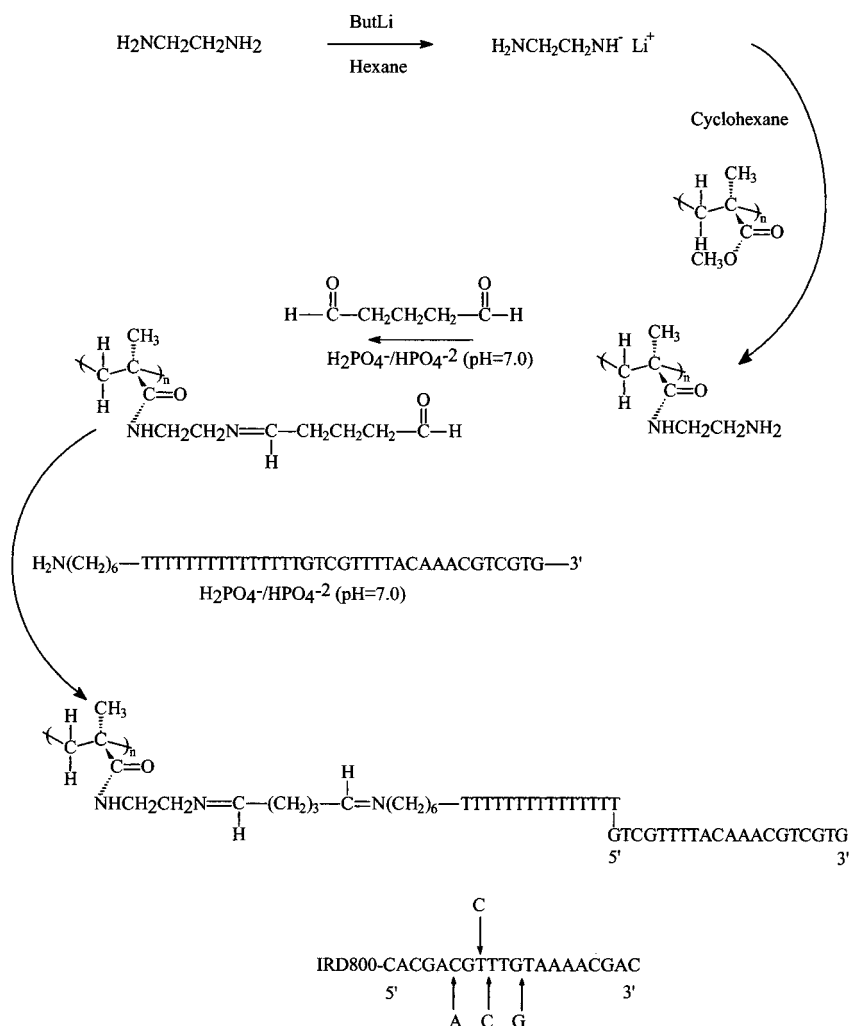
Data analysis functionality was integrated directly into the controlling software. The data in the compressed binary file with the pixel decay information could be displayed as an entire 2D image of both the fluorescence intensity and lifetime or along one line horizontally or vertically across the image, which was selected with cursors. The decay profiles for each pixel or series of pixels could be selected using a pair of cursors from the 2-D image. After construction of the decay profile, the lifetime was calculated directly using eq 1 (see below).

For excitation at 488 nm, an air-cooled argon ion laser (OmniChrome model 532, Chino, CA) was used for excitation. The optical setup was similar to that for the NIR except that the excitation beam was passed through a 495-nm dichroic filter (495DRLP, Omega Optical) and focused onto the solid substrate using a 40 \times microscope objective. A long-pass filter (cut on wavelength = 510 nm, Newport Corporation) and a band-pass filter with a center wavelength of 515 nm (515DF10, Omega Optical) were used to block out any stray light or scatter.

Fluorescence Measurements of Spotted Dyes on Slides.

Fluorescence measurements were performed by spotting NN382 or $\text{AlNc}(\text{SO}_3^-)_4$ on the surface of the appropriate substrate in a grid pattern defined by a piece of paper placed under the transparent substrate. Each element of the grid measured 2 mm \times 2 mm (5 \times 5 array). The dyes were dissolved in DMSO and spotted onto the surface using a 25 μm i.d. capillary. The total volume of dye deposited for each spot was estimated to be approximately 1.0 μL , with the diameter of the spot being approximately 2 mm. After being spotted, the slides were either

Scheme 1



allowed to dry (in the dark) under a stream of N_2 or covered with a cover slip.

Covalent Attachment of Oligonucleotides to PMMA and Hybridization Assays. The covalent attachment of the oligonucleotides to PMMA was accomplished by using the procedure depicted in Scheme 1.³² Oligonucleotide hybridization experiments were performed on PMMA slides cut into 30 mm \times 50 mm rectangles. Before preparation, the PMMA slides were soaked in a 10/90 methanol/water solution (v/v) for thirty minutes, rinsed with triply distilled water, and dried with compressed air. A lithium ethylenediamine solution was prepared by agitating *n*-butyllithium, cyclohexane, and ethylenediamine in a vortex mixer for thirty minutes. The cleaned PMMA sheets were then agitated with the lithium ethylenediamine solution and cyclohexane, which resulted in the attachment of the diamine to the PMMA surface through the formation of an amide bond. After being washed with deionized water, the PMMA slide was placed in a 5% glutaraldehyde-phosphate buffer ($\text{H}_2\text{PO}_4^-/\text{HPO}_4^{2-}$) solution for 5 h at a pH of 7.0. The slides were then spotted with the amino-modified oligonucleotides, using a quill pen, to the derivatized PMMA by Radius Biosciences (Medfield, MA). The arrays contained 24

spots, with each spot possessing a diameter of $\sim 400 \mu\text{m}$ (deposition volume = 10 nL) and a center-to-center spacing of $600 \mu\text{m}$. Following oligonucleotide attachment, the residual free-aldehyde groups were capped with ethanol amine to prevent nonspecific adsorption of the target oligonucleotide to the substrate. The slides were air-dried and stored in a freezer (-20°C) until required for use.

For the hybridization assays, a 100 nM solution of an IRD800-labeled complementary target (Li-COR Biotechnology), $5\times$ saline-sodium phosphate EDTA (SSPE), and 0.5% sodium dodecyl sulfate (SDS) were placed over the array, and hybridization was allowed to proceed for thirty minutes in the dark at 30°C in a humidified chamber. Following hybridization, the PMMA slide was washed extensively with $5\times$ SSPE–0.5% SDS solution for 15 min (repeated 5 times) and was allowed to dry under a stream of N_2 . Fluorescence measurements were made on dried PMMA slides.

Surface Quantification of Oligonucleotides on PMMA. Quantification of the number of surface-bound oligonucleotides on the PMMA slides was determined using a ^{32}P -labeled, 5'-amino modified oligonucleotide (5' $\text{H}_2\text{N}(\text{CH}_2)_6\text{-TTTTTTTTTTTGTGTCGTTTACAAACGTCGTG-3'}$). The 35mer was labeled using an [$\alpha\text{-}^{32}\text{P}$]ddATP 3'-end labeling kit obtained from Amersham-Pharmacia Biotechnology (Arlington Heights, IL), which had a

(32) Henry, A. C.; Tutt, T. J.; McWhorter, C. S.; Davidson, Y. Y.; Galloway, M.; Soper, S. A.; McCarley, R. L. *Anal. Chem.* (accepted for publication, 2000).

Table 2. Number of Background Photons Coupled into the NIR TCSPC Imager from Various Substrates at 488 and 780 nm Excitation Wavelengths

material	background (cps)	
	488 nm	780 nm
PMMA	103 000	42 000
glass	76 000	51 000
poly-L-lysine	135 000	84 000

In both cases, 0.3 mW of laser power was focused onto the substrate surface using a 40 \times objective.

specific activity of 5000 Ci/mmol. The reaction consisted of 2.1 $\times 10^{-13}$ moles of the amino-modified single-stranded 35mer, 2.1 $\times 10^{-13}$ moles of the ^{32}P -labeled *dd*ATP, and 10 units of the terminal transferase enzyme. The reaction volume was taken to 50 μL by adding cacodylate buffer made up in *ddH*₂O. Purification of the labeled oligonucleotide was accomplished using a Microspin G-25 column (Amersham Pharmacia). Following purification, the efficiency of the labeling reaction (determined through scintillation counting) was found to be 52% ($\pm 3\%$). The purified ^{32}P -labeled 35mer was covalently attached to the functionalized PMMA-surface using the procedures described above. Following the attachment reaction, the PMMA surface was washed 5 times with a 1% solution of NH_4OH , and subsequent washings with copious amounts of *ddH*₂O. Scintillation counting was performed using a Beckman LS6000 scintillation counter (Beckman Instruments, Fullerton, CA) and the surface concentration obtained from the specific activity of the probe and the measured activity of the slide.

Fluorescence Lifetime Calculations. The lifetimes of the array spots or image pixels were calculated using maximum likelihood estimators^{30,33}

$$1 + (e^{T/\tau_f} - 1)^{-1} - m(e^{mT/\tau_f} - 1)^{-1} = N_t^{-1} \sum_{i=1}^m iN_i \quad (1)$$

where N is the total number of photocounts in the decay profile, T is the time width of each bin (24.4 ps), m is the time interval over which the lifetime was calculated (25 ns), i is the time bin number, and N_i is the number of counts in the i^{th} time bin. The standard deviation in the measurement using this relationship is simply given by $\tau_f \times N^{-(1/2)}$, where τ_f is the calculated fluorescence lifetime. The use of this expression allowed the determination of only a single lifetime, even in the case of multiexponential decays.

RESULTS AND DISCUSSION

Array Substrate Backgrounds. One of the analytical challenges in reading fluorescence from DNA microarrays is the limited amount of material that must be interrogated due to the low loading level of fluorochromes to the array surface. Therefore, low background levels should be produced from the array to improve the SNR in the measurement. The background signals can result either from specularly scattered light or autofluorescence generated from the immobilization substrate or the material deposited onto it. In Table 2 are shown background signals

measured from different array materials when they are excited in the visible (488 nm) or NIR (780 nm) regions. The glass slide yielded the least amount of background (76 000 cps) when excitation was performed at 488 nm, while the glass slides coated with poly-L-lysine, a widely used substrate for array applications because of its ability to bind DNA efficiently,³⁴ yielded the highest background level (135 000 cps). As can be seen from Table 2, the background signal was lower in all cases for NIR excitation. The lower background signal level was attributed to the limited number of fluorophores that fluoresce in the NIR as well as the reduced number of scattering photons generated due to the smaller Raman cross-sections observed in the NIR.

Because we were interested in measuring fluorescence lifetimes on these substrates, the time distribution of the background photons was then acquired at 780 nm excitation to determine if any residual fluorescence was produced by the substrate which would affect the lifetime measurement. Figure 2 depicts the decay profiles for PMMA, glass, and poly-L-lysine slides. As can be seen from this figure, the scattering peaks, which were produced from photons coincident with the laser pulse, observed for glass and poly-L-lysine were superimposed on a relatively large and flat background. However, this constant background was not seen in the case of PMMA. This background was believed to arise from some long-lived luminescent species present in glass that could be efficiently excited at 780 nm but which was absent in PMMA. Therefore, PMMA not only resulted in a lower absolute intensity in the background signal, but also the photon distribution indicated that their origination was predominantly from scattering effects. The formal width at half-maximum for the prompt peak shown for PMMA provides information on the time response of the instrument and was found to be 275 ps. It has been shown that small photoactive-area single-photon avalanche diodes, while producing favorable timing responses for TCSPC measurements, are sensitive to minor defocusing in terms of their timing behavior.^{35,36} However, we found that the half-width of the instrument response function did not change by more than 10% during translational movements of the scanner across the surface being imaged.

Steady-State and Time-Resolved NIR Fluorescence of Dyes Deposited on PMMA. The dynamic range and limit of detection of two different NIR dyes on PMMA were then determined for solutions of IRD800 and $\text{AlNc}(\text{SO}_3^-)_4$ directly spotted onto the surface, with the fluorescence intensity recorded as a function of scan position. It was anticipated that some dye-stacking was occurring, especially at the higher deposition concentrations. In this case, the dimers or other higher order aggregates would be expected to produce a smaller amount of fluorescence due to reduced quantum yields as compared to the monomers.^{37,38} The intensity response of the imager was found to be linear from 1.0 pM to 10 nM, with a correlation coefficient of 0.992 for both IRD800 and $\text{AlNc}(\text{SO}_3^-)_4$. The SNR at a deposition concentration of 1.0 pM for IRD800 was determined

(34) Nguyen, Q.; Heffelfinger, D. M. *Anal. Biochem.* **1995**, 226, 59–67.

(35) Li, L.-Q.; Davis, L. *Rev. Sci. Instr.* **1993**, 64, 1524–1529.

(36) Cova, S.; Longoni, A.; Ripamonti, G. *IEEE Trans. Nucl. Sci.* **1982**, NS-29, 599–601.

(37) Makio, S.; Kanamaru, N.; Tanaka, J. *Bull. Chem. Soc. Jpn.* **1980**, 53, 3120–3124.

(38) Waddell, E. A.; Stryjewski, W.; Soper, S. A. *Rev. Sci. Instr.* **1998**, 70, 32–37.

(33) Hall, P.; Selinger, B. *J. Phys. Chem.* **1981**, 45, 2941–2946.

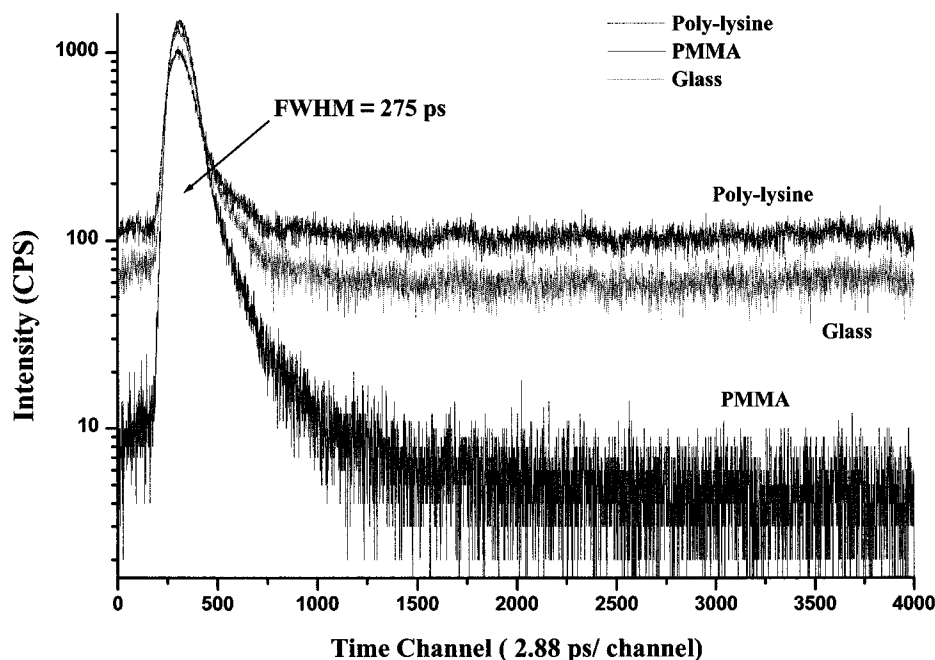


Figure 2. Decay profiles for glass, PMMA, and poly-L-lysine-coated glass slides. The slides were excited with 0.4 mW (average power) at 780 nm operating at a repetition rate of 40 MHz. The accumulation time for each decay profile was 10 s, and the slides were linearly scanned at approximately 127 $\mu\text{m/s}$ to avoid photobleaching effects.

to be 8.0. This corresponds to a concentration LOD of 0.38 pM. The molecular surface concentration (C_{surf}), assuming no dye stacking (valid at low deposition concentrations), may be determined from

$$C_{\text{surf}} = (C \times V \times N_A) / A \quad (2)$$

where C is the solution dye concentration (moles/L), V is the volume of the drop (L), N_A is Avogadro's number (6.022×10^{23} molecules/mole), and A is the area of the spot (cm^2). At 0.38 pM, the surface concentration was calculated to be 2.9×10^5 molecules per mm^2 (0.29 fluors/ μm^2). Similar experiments were also performed for $\text{AlNc}(\text{SO}_3^-)_4$, with an LOD found to be 9.53 fluors/ μm^2 . Inspection of the photophysical parameters listed in Table 1 would indicate that $\text{AlNc}(\text{SO}_3^-)_4$ should demonstrate a lower LOD due to its superior quantum yield and higher photochemical stability. The poorer molecular LOD may have resulted from the filter set of the imager that was not optimized for this particular dye due to its small Stokes' shift and narrow emission band.

A primary concern for implementing NIR dyes in microarray applications is the potentially poor photochemical stability of these dyes when they are deposited onto substrates and irradiated with high laser fluences. Because the data depicted in Table 1 were acquired on dyes in solution (DMSO), we measured the bleaching rate of these dyes when deposited onto PMMA and dried (measured in air) and compared these bleaching rates to those observed in DMSO. The bleaching decays for both IRD800 and $\text{AlNc}(\text{SO}_3^-)_4$ on PMMA and in DMSO are shown in Figure 3. Qualitatively, we observed that the bleaching of IRD800 was faster than that seen for $\text{AlNc}(\text{SO}_3^-)_4$, which is consistent with the solution-phase results shown in Table 1. The bleaching curves depicted in Figure 3 for the dyes deposited onto PMMA were fit to either single or double exponentials from which the photobleaching quantum efficiencies could be extracted. The photo-

bleaching quantum efficiency for $\text{AlNc}(\text{SO}_3^-)_4$ was found to be 2.6×10^{-6} on PMMA (dry), but for IRD800, the rate was 7.3×10^{-6} (dry). As can be seen from these numbers, $\text{AlNc}(\text{SO}_3^-)_4$ exhibited a better photochemical stability, as compared to IRD800, which is similar to what was observed in solution. It should be noted that for both dyes that were deposited onto PMMA and measured in the dry state, the curves were more adequately fit to a double exponential, which is consistent with multiple bleaching pathways or multiple species being monitored. The second photobleaching quantum efficiencies obtained from these curves were 2.7×10^{-7} for $\text{AlNc}(\text{SO}_3^-)_4$ and 6.2×10^{-7} for IRD800. Although we could not extract the exact photon numbers per molecule, due to the inability to determine the fluorescence quantum yields for the dyes deposited onto PMMA, it is clear that in the dry state, both dyes demonstrate greater photochemical stability.

To evaluate the ability of the system to identify analytes through the use of fluorescence lifetimes, a time-resolved analysis of 1.0 nM $\text{AlNc}(\text{SO}_3^-)_4$ and IRD800 deposited onto PMMA were conducted. These experiments were performed by depositing dye solution (in DMSO) directly onto PMMA and allowing it to dry. Fluorescence was then collected at a low scan rate to minimize photodegradation, and the histograms were analyzed using a nonlinear least-squares fitting algorithm (FLA-900, Edinburgh Instruments, Livingston, U.K.) to assess the exponential composition of the decays (mono- or multiexponential). Analysis of the decay data indicated that IRD800 possessed a lifetime of 1.21 ns ($\chi^2 = 1.33$), whereas $\text{AlNc}(\text{SO}_3^-)_4$ possessed a lifetime of 1.90 ns ($\chi^2 = 1.42$). At this concentration, the decays were adequately fit to single-exponential functions. However, at higher concentrations (>10 nM), the decays did show deviations from a single-exponential function. The lifetime obtained for the $\text{AlNc}(\text{SO}_3^-)_4$ was much shorter than the value obtained in bulk solution, which

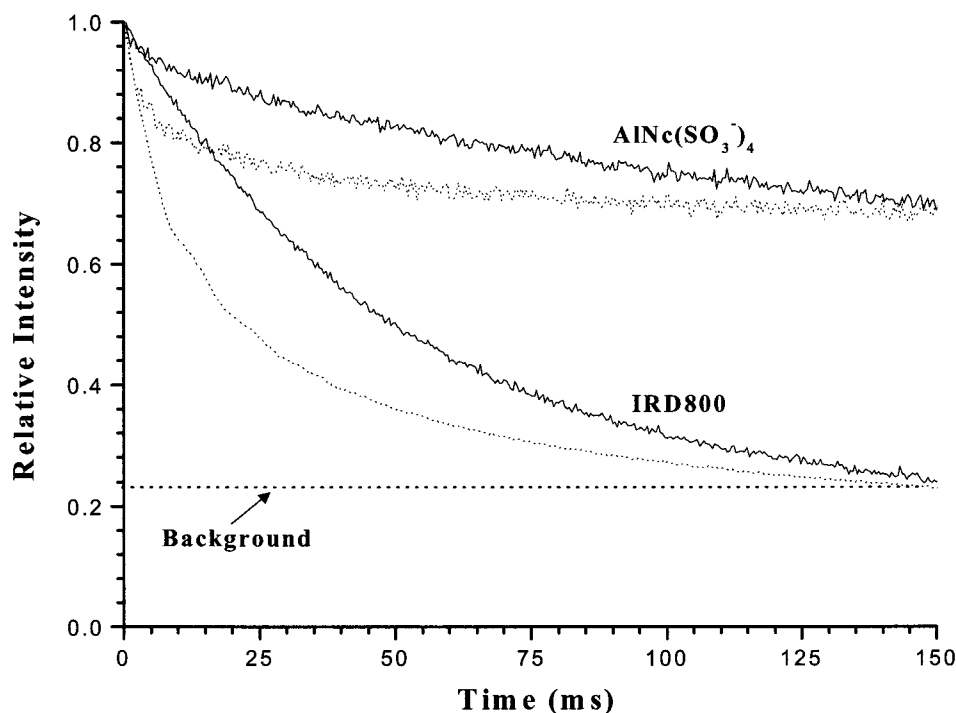


Figure 3. Photobleaching curves for IRD800 and $\text{AlNc}(\text{SO}_3^-)_4$ spotted directly onto PMMA. The dye deposition volume was $1.0 \mu\text{L}$, and the solvent was DMSO, with the dye concentration in all cases being 1.0 nM . For the wet measurements (solid lines), the dye was deposited onto the slide, a coverslip was placed over the spot, and the spot immediately positioned under the imager with the laser off. Once positioned, the laser was turned on, and timed data acquisition commenced. For the dry measurements (dotted lines), the slides were allowed to dry under a stream of N_2 in the dark prior to measurement. The average laser power was set at 0.4 mW (laser fluence = $1.1 \times 10^{22} \text{ photons s}^{-1} \text{ cm}^{-2}$). The dashed line represents the relative background contribution to the observed signal.

was found to be 2.92 ns (DMSO).³⁸ However, the lifetime for IRD800 was much longer on the PMMA surface in a dry state as compared to that measured in bulk solution (0.76 ns , DMSO). The differences that were observed between the lifetimes measured on a dry surface and those obtained in bulk solution may have been due to differences in their microenvironments because these dyes have been shown to be very sensitive to their immediate environment.³⁹ The longer lifetime for IRD800 is most likely a result of the fact that the major nonradiative manifold results from a time-dependent internal conversion rate, which depends on the rate of conformational changes occurring in the excited state.^{39–41} In the solid state, these conformational changes are effectively impeded, lowering the rate of nonradiative internal conversion and, thus, increasing the fluorescence lifetime.

Surface Coverage of Oligonucleotides on PMMA. The amount of tethered oligonucleotide to the PMMA surface was assessed using a ^{32}P -labeled oligonucleotide and scintillation counting. The glutardialdehyde-functionalized PMMA slide was reacted with the ^{32}P -labeled oligonucleotide, inserted into a scintillation cocktail, and the activity was measured to determine the amount of DNA covalently attached to the surface. The volume of deposited DNA was $1.0 \mu\text{L}$, and the spot possessed a diameter of 1.5 mm , as determined through inspection using an optical microscope. Following extensive washing of the slide, the measured activity allowed determination of the amount (moles) of

DNA tethered to the surface, and from the diameter of the deposited spot, the surface concentration could be determined. The surface concentration of the 35mer was estimated to be $3.31 \times 10^{-22} \text{ moles}/\mu\text{m}^2$ ($3.31 \times 10^{-14} \text{ moles}/\text{cm}^2$) or approximately $400 (\pm 25)$ molecules per μm^2 . The amount of ssDNA that could be attached to the surface was determined by a number of factors, including (1) the number of methyl ester groups accessible in the PMMA polymer backbone, (2) the efficiency in the formation of the amine foundation layer, (3) the efficiency in the attachment of glutardialdehyde to the aminated PMMA, (4) the number of accessible aldehyde groups to the amine-modified oligonucleotide, and (5) the efficiency in the reaction of the ssDNA to the aldehyde groups present on the PMMA surface. Recently, we found that the surface concentration of primary amine groups formed using our amination-modification chemistry of PMMA was $6.85 \text{ nmol}/\text{cm}^2$, as determined by using X-ray photoelectron spectroscopy.³² This value is indicative in the efficiency of points 1 and 2 that were cited above. Therefore, the combined efficiency of the subsequent steps, 3–5, was only $(4.8 \times 10^{-4})\%$. We suspect that part of this low efficiency is due to the instability of the imine-bond that is formed between the primary amine and the aldehyde, attachment of both aldehyde groups of glutardialdehyde to the aminated-PMMA and/or inaccessibility of the oligonucleotide to the glutardialdehyde-functionalized PMMA surface.

DNA Hybridization on PMMA Substrates with Time-Resolved NIR Fluorescence. We next carried out hybridization studies of NIR-labeled oligonucleotide complements and non-complements to DNA covalently attached to our appropriately prepared PMMA surfaces. The results of these experiments are

(39) Soper, S. A.; Mattingly, Q. L. *J. Am. Chem. Soc.* **1980**, *53*, S **1994**, 116, 3744–3752.

(40) Martin, M. *Chem. Phys. Lett.* **1975**, *35*, 105–111.

(41) Siebrand, W.; Williams, D. F. *J. Chem. Phys.* **1968**, *49*, 1860–1871.

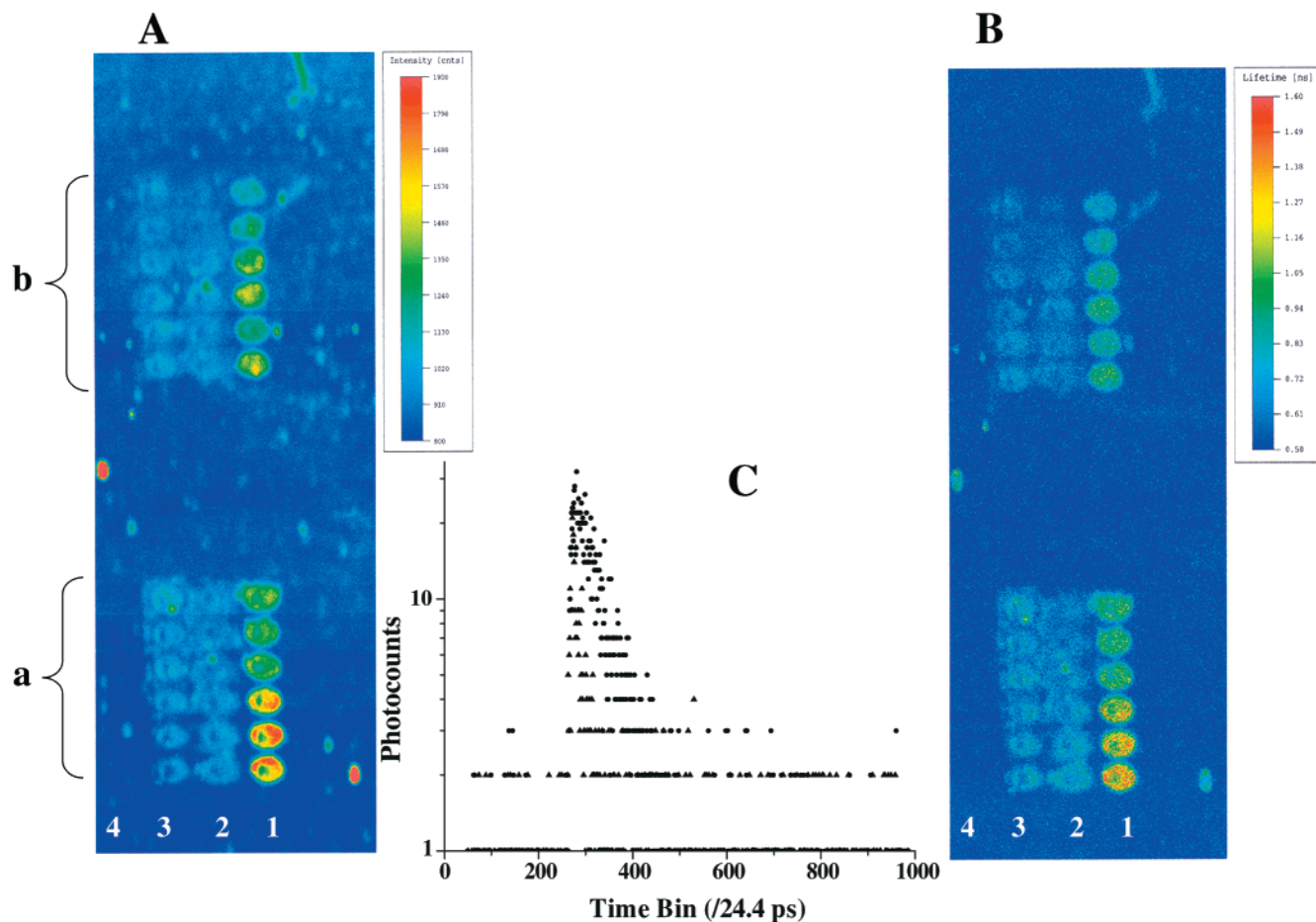


Figure 4. Fluorescence intensity image (A) and lifetime image (B) of two 4×6 DNA microarrays (a and b). The PMMA slides were derivatized using glutaraldehyde, and then the probe DNA was spotted onto the PMMA using quill spotting. The spots were approximately $400 \mu\text{m}$ in diameter with a center-to-center spacing of $600 \mu\text{m}$. (C) Decay profiles for background signals generated from PMMA (triangles) and a hybridization spot (array a, column 1, circles) for a single image pixel. The arrays were scanned at a speed of $127 \mu\text{m/s}$ and an accumulation time per pixel of 0.1 s . The laser was tuned to 780 nm with a repetition frequency of 40 MHz and an average power at the surface of 0.4 mW . The arrays were completely covered with a 100.0 nM solution of the labeled complement and allowed to hybridize at 30°C for 30 min . The intensity and lifetime scales of the image were selected by averaging the background or lifetime over nonhybridization pixels (lower limit) and pixels that resulted in the maximum intensity or lifetime (upper limit). The columns in each array represent a fully matched duplex (column 1), three-base mismatch (column 2), single-base mismatch (column 3), and a complete mismatch (column 4). See Scheme 1 for position of mismatches. The images represent raw images.

depicted in Figures 4 and 5, with Figure 4A showing the intensity image and Figure 4B showing the lifetime image of two 4×6 DNA microarrays. To acquire the images, the scanner was moved in $12.7 \mu\text{m}$ steps, and the integration time per pixel was 0.1 s . From the data shown for both the intensity and lifetime images, it was determined that each spot was circular, with an average diameter of 35 pixels (spot diameter = $444 \mu\text{m}$). In these experiments, four columns (six spots per column) are present in the array: (1) fully matched duplexes, (2) three-base mismatch (up arrows, see Scheme 1), (3) one-base mismatch (down arrow, see Scheme 1), and (4) fully mismatched duplexes. As can be seen from the intensity or lifetime image, little nonspecific adsorption of DNA to the aminated-PMMA surface was observed. In addition, using our hybridization conditions, the fluorescence intensity (see Figures 4A and 5A) for column 1 (fully matched duplexes) was higher than that seen in columns 2–4.

By integrating the background-corrected intensity (background-corrected with respect to column 4) over each spot of the array (1018 pixels), the average intensity was determined to be $8.1 (\pm$

$2.0) \times 10^5$ counts for column 1, $3.8 (\pm 0.4) \times 10^5$ counts for column 2, and $4.1 (\pm 0.3) \times 10^5$ counts for column 3. Using the background-corrected counts for only column 1 and the integrated background counts per spot (7.6×10^5), the SNR was found to be 9.3×10^2 , where the SNR was calculated from $\text{SNR} = S/(B)^{1/2}$, where S is the background-corrected signal and B is the background. If we assume that all available anchoring sites on the PMMA-functionalized surface were occupied by labeled-oligos, the surface concentration of oligos was $3.31 \times 10^{-22} \text{ moles}/\mu\text{m}^2$ (see above). Therefore, each spot (area = $1.6 \times 10^5 \mu\text{m}^2$) contains $5.1 \times 10^{-17} \text{ moles}$ of labeled oligonucleotides. Our estimated mass detection limit (SNR = 2) for a typical array spot on PMMA using NIR fluorescence detection following DNA hybridization would be $1.0 \times 10^{-19} \text{ moles}$ ($0.38 \text{ molecules}/\mu\text{m}^2$), which is similar to what we found for dyes directly spotted onto PMMA. This result indicates that the materials used for hybridization do not exhibit appreciable fluorescence when excited at 780 nm . It has been shown that a 40-fold degradation in the LOD has been observed for 488 nm excitation of fluorescein-labeled oligonucle-

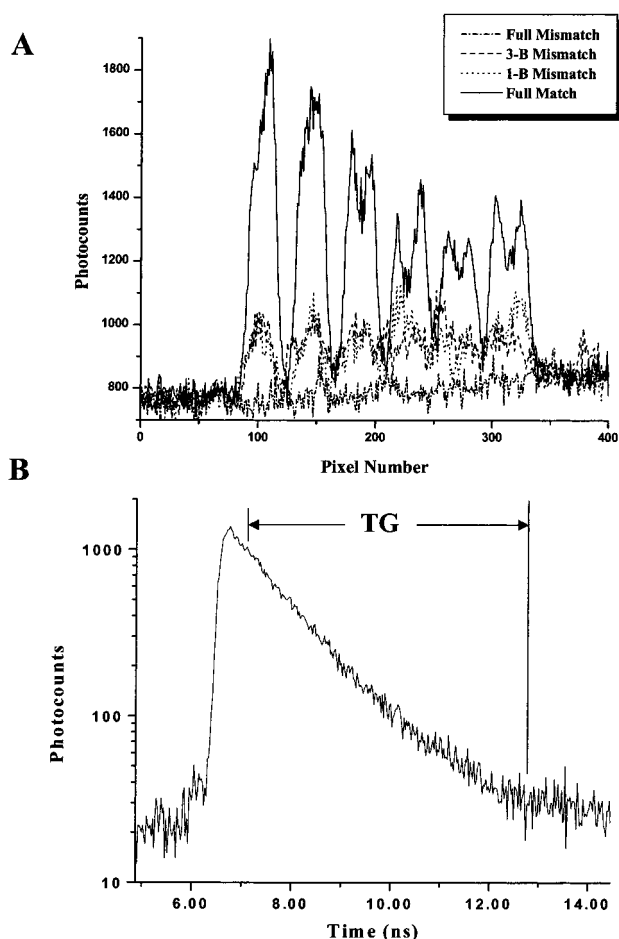


Figure 5. (A) Fluorescence intensity of the 4 columns of the DNA microarray (perfect match, 1-base mismatch, 3-base mismatch, and fully mismatched duplexes) interrogated using time-resolved NIR fluorescence. The intensity represents one pixel taken from the center of each column of array a (see Figure 4A). (B) Decay profile taken from a complete-matched hybridization spot (column 1, array a, see Figure 4A). The decay was constructed from 48 pixels centered on one of the hybridization spots. See Figure 4 for experimental details.

otides following hybridization to their complements tethered to glass, as compared to direct deposition of the labeled oligos onto glass.⁶

We also obtained the image of this hybridization array using time-gated detection. The position of the time-gate was selected to effectively discriminate the scattered photons from the fluorescence photons (see Figure 5B). When the array was re-imaged using time-gated detection (data not shown), we found that the SNR improved 10-fold ($\text{LOD} = 0.038 \text{ fluors}/\mu\text{m}^2$), as compared to the SNR obtained for the image depicted in Figure 4A.

We next carried out a lifetime analysis during imaging using maximum likelihood estimators (see eq 1), and this lifetime image is shown in Figure 4B. Comparison of the lifetime image to the intensity image over the entire array surface showed qualitatively that the lifetime image was much cleaner in terms of fewer high-intensity/lifetime spots, which show up in nonhybridization pixels of the image. These spots arise from imperfections in the substrate material, which scatter light and increase the intensity at that pixel. However, in the lifetime image, these spots do not show up, due to the fact that the calculated lifetime is partially immune to scattering increases because the time distribution of these photons

is coincident with the laser pulse, and the lifetime was calculated over a time interval in which the scattered photon contribution to the decay is minimal. We also noticed that the lifetime image contained a wide spread of values when we compared the lifetimes of spots between columns. Because the only distinction between columns is the number of labeled targets present in a spot resulting from mismatches, we would anticipate similar lifetime values between columns of the array due to the concentration-independent behavior of the lifetime when implementing lifetime imaging techniques.^{42,43} As can be seen in Figure 4C, the number of photons in the fluorescence decay (accumulated on a single pixel) was small (~ 1550 counts), and the background makes a significant contribution to the resulting decay. Because our algorithm makes no distinction between multiexponential decays and single exponential decays, the poor photon statistics and large background contribution biases in the lifetime determination resulted in the lifetime discrepancies observed between columns.²⁸

A typical decay profile for the IRD800 NIR labeled-duplex is shown in Figure 5B, which was constructed by integrating over 48 pixels (6×8) centered on a spot of the array, to improve the photon statistics. In all cases, the decays were found to be linear, which is consistent with a single species producing the fluorescence. This is to be expected because the surface coverage is low and the NIR labels are strongly bound to the anchored DNAs, preventing any type of dye-stacking. Calculation of the lifetimes for the spots that are shown in column 1 yielded an average value of $1.23 (\pm 0.01)$ ns, a value that is similar to what was found for this dye directly deposited onto PMMA. The average number of counts that were included in the calculation was 48 800. If the precision in the lifetime measurement is determined solely by photon statistics, then the standard deviation in the measurement can be determined, when using maximum-likelihood estimators, from $\tau_f \times N_t^{-1/2}$. On the basis of the total number of counts included in the calculation and the observed lifetime, the standard deviation was calculated to be 0.005 ns, which is in close agreement to that determined from replicate lifetime measurements (0.01 ns) and indicates that the precision in our lifetime values was determined primarily by photon statistics. The image depicted in Figure 4B shows a greater spread in the lifetime values within a single spot, as would be anticipated on the basis of the measured standard deviations. This results from the fact that the number of photons analyzed per pixel is substantially reduced as compared to the case when multiple pixels are analyzed in one hybridization spot. For example, if the decays for the 12 spots of column 1 are analyzed on a per-pixel basis (48 pixels per spot), the average lifetime value becomes 1.0 ns, and the standard deviation is 0.2 ns ($\text{RSD} = 20\%$), a substantially lower precision and shorter lifetime. On the basis of the average number of photons per pixel in a hybridization spot of column 1 (~ 1550), the predicted photon statistical standard deviation would be 0.3 ns, which is in close agreement with that determined above.

We also measured the lifetime values for columns 2 and 3 in our hybridization arrays. For column 3 (single-base mismatch), the average lifetime value was $1.17 \text{ ns} (\pm 0.03)$, and for column 2 (three-base mismatch), the average lifetime value was determined

(42) Lakowicz, J. R.; Szmajcinski, H.; Nowaczyk, K.; Johnson, M. L. *PNAS* **1992**, *89*, 1271–1275.

(43) Lakowicz, J. R.; Szmajcinski, H.; Nowaczyk, K.; Berndt, K. W.; Johnson, M. *Anal. Biochem.* **1992**, *202*, 316–330.

to be 1.12 ns (± 0.03). We noticed that the decays in these cases were somewhat nonlinear in the earlier time regions of the histogram, which is indicative of a high number of scattering photons being accumulated into the decay, which biases the lifetime to somewhat lower values.²⁸ Because the mismatches in these examples were located in the center of the duplex (see Scheme 1), the duplexes that did form were suspected of having comparable microenvironments near the dye termini. Therefore, the lower lifetime arising from the mismatched DNA is most likely a consequence of a smaller signal-to-background ratio and not a consequence of alterations in the dye's microenvironment produced by mismatches.

CONCLUSIONS

We have built and characterized a device for NIR time-resolved fluorescence detection and imaging of solid surfaces for reading fluorescence signatures, both steady-state and time-resolved, from DNA microarrays. The timing response of this device was found to be 275 ps, which is adequate for determining subnanosecond fluorescence lifetimes. Additionally, we found that the LOD of this device was 0.38 molecules/ μm^2 and could be improved by a factor of 10 if using time-gated detection. The lifetime analysis of NIR dyes deposited directly onto PMMA indicated that the decays were described by single exponential functions, with lifetime values that differed from those in bulk solution. Using glutardialdehyde linkage chemistry, oligonucleotide probes could be covalently tethered to an aminated-PMMA surface and used for capturing complements with single-base discrimination, as discerned from the fluorescence intensity that is produced from the hybridization events. In addition, the lifetimes could be determined for pixels of the array using maximum likelihood estimators. The lifetime of IRD800-captured complements was found to be 1.23 ns, which is longer than the lifetime measured in bulk solution.

Although NIR fluorescence is an attractive alternative to visible fluorescence for reading microarrays, improvements in measurement sensitivity can be realized using the selection of labeling fluorochromes that possess higher fluorescence quantum yields and better photobleaching stabilities. The present application used the tricarboyanines for monitoring hybridization events because of their accessibility. However, use of the $\text{AlNc}(\text{SO}_3^-)_4$ will further improve the LOD for NIR fluorescence due to their better photochemical properties using the appropriately designed imager (correct choice of filtering optics). Work is currently underway in our laboratory to make such labeling analogues.

In addition, polymers with accessible functional groups can serve as attractive substrate materials for tethering oligonucleotides for array applications. PMMA resulted in a lower absolute background signal as compared to glass due to the absence of some unknown long-lived luminescent species observed for glass when it was excited at 780 nm. Another attractive feature of polymers is their ease in fabricating microfluidic devices. As such, one can envision microfluidic devices constructed from polymers and containing tethered oligonucleotide probes for capturing DNAs. This arrangement would reduce the hybridization volume and allow forced convection to reduce the hybridization kinetics typically seen in conventional high-density array formats.

ACKNOWLEDGMENT

The authors thank the National Institutes of Health (R01-01499, R23-CA84625) and FMC BioProducts (Rockport, ME) for financial support of this work. E.A.W. also thanks the National Institutes of Health for supplying a pre-doctoral fellowship for support of his work.

AC0009705